BRAIN
A JOURNAL OF NEUROLOGY

Autism-associated 16p11.2 microdeletion impairs prefrontal functional connectivity in mouse and human

Alice Bertero,[1,2,*] Adam Liska,[1,*] Marco Pagani,[1,*] Roberta Parolisi,[3]
Maria Esteban Masferrer,[4] Marta Gritti,[5] Matteo Pedrazzoli,[5] Alberto Galbusera,[1]
Alessia Sarica,[6] Antonio Cerasa,[6,7] Mario Buffelli,[8] Raffaella Tonini,[5] Annalisa Buffo,[3]
Cornelius Gross,[4] Massimo Pasqualetti[1,2] and Alessandro Gozzi[1]

*These author contributed equally to this work.

Human genetic studies are rapidly identifying variants that increase risk for neurodevelopmental disorders. However, it remains unclear how specific mutations impact brain function and contribute to neuropsychiatric risk. Chromosome 16p11.2 deletion is one of the most common copy number variations in autism and related neurodevelopmental disorders. Using resting state functional MRI data from the Simons Variation in Individuals Project (VIP) database, we show that 16p11.2 deletion carriers exhibit impaired prefrontal connectivity, resulting in weaker long-range functional coupling with temporal-parietal regions. These functional changes are associated with socio-cognitive impairments. We also document that a mouse with the same genetic deficiency exhibits similarly diminished prefrontal connectivity, together with thalamo-prefrontal miswiring and reduced long-range functional synchronization. These results reveal a mechanistic link between specific genetic risk for neurodevelopmental disorders and long-range functional coupling, and suggest that deletion in 16p11.2 may lead to impaired socio-cognitive function via dysregulation of prefrontal connectivity.

1 Functional Neuroimaging Laboratory, Istituto Italiano di Tecnologia, Center for Neuroscience and Cognitive Systems @UniTn, Rovereto, Italy
2 Department of Biology, Unit of Cell and Developmental Biology, University of Pisa, Pisa, Italy
3 Department of Neuroscience Rita Levi-Montalcini- University of Torino, Neuroscience Institute Cavalieri Ottolenghi (NICO), Torino, Italy
4 Epigenetics and Neurobiology Unit, European Molecular Biology Laboratory (EMBL), Monterotondo, Italy
5 Neuroscience and Brain Technologies Department, Istituto Italiano di Tecnologia, Genova, Italy
6 Consiglio Nazionale delle Ricerche, Catanzaro, Italy
7 S. Anna Institute and Research in Advanced Neuro-rehabilitation (RAN) Crotone, Italy
8 Department of Neurosciences, Biomedicine and Movement Sciences, University of Verona, Italy

Correspondence to: Alessandro Gozzi
Functional Neuroimaging Laboratory,
Center for Neuroscience and Cognitive Systems @ UniTn,
Istituto Italiano di Tecnologia,
38068, Rovereto, Italy
E-mail: alessandro.gozzi@iit.it

Abbreviations: ASD = autism spectrum disorder; CNV = copy number variation; EPSC = excitatory postsynaptic current; PFC = prefrontal cortex; rsfMRI = resting state functional MRI; SRS = social responsiveness scale

Introduction

Over the past decade significant strides have been made toward understanding the genetic basis of autism spectrum disorders (ASDs) and related heritable neurodevelopmental conditions (Chen *et al.*, 2015; Tick *et al.*, 2016). The identification of several gene variants and mutations associated with increased ASD risk (de la Torre-Ubieta *et al.*, 2016) has advanced our understanding of ASD mechanisms, by providing a platform for unravelling the causal chain of events that result in ASD. However, great challenges remain in delineating how heterogeneous genetic forms of ASDs might converge into circuital and behavioural alterations characteristic of this cluster of disorders.

Chromosomal copy number variations (CNVs) have been associated with 5–10% of patients with ASD (de la Torre-Ubieta *et al.*, 2016). Microdeletion of human chromosome 16p11.2 is one of the most common CNVs in ASD, accounting for ∼0.5–1% of all cases (Kumar *et al.*, 2008; Malhotra and Sebat, 2012). The affected region encompasses ∼29 annotated protein-coding genes, many of which are expressed in the brain (Blumenthal *et al.*, 2014). Previous studies have demonstrated that ASD is diagnosed in ∼18% of 16p11.2 deletion carriers and that this CNV affects global cognition by resulting in a highly penetrant reduction in intelligence quotient (IQ, Zufferey *et al.*, 2012). Importantly, human neuroimaging investigations in children with the 16p11.2 deletion have revealed brain structural abnormalities affecting grey matter areas previously implicated in ASD (Qureshi *et al.*, 2014; Maillard *et al.*, 2015). Deletion in syntenic regions to 16p11.2 in animals results in neural apoptosis deficits and increased neuronal progenitor proliferation (Golzio *et al.*, 2012; Pucilowska *et al.*, 2015), suggesting a role of precocious molecular and cellular events in the establishment of deviant brain morphoanatomy associated with 16p11.2 deletion. However, it remains unclear whether and how these neuroanatomical alterations affect brain function, and what brain substrates are primarily affected.

Mounting evidence points at a role for aberrant functional connectivity in the resting state as a hallmark feature of ASD (Di Martino *et al.*, 2014). However, great heterogeneity exists in the manifestation of abnormal connectivity across studies and, besides a few notable exceptions (Scott-Van Zeeland *et al.*, 2010; Rudie *et al.*, 2012), attempts to relate individual ASD genetic aetiologies to specific connectional or circuital dysfunctions have been lacking. In the present work we mapped functional connectivity in a genetically defined cohort of 16p11.2 deletion carriers (Simons VIP Consortium, 2012) as assessed with resting state functional MRI (rsfMRI). We show that 16p11.2 deletion impairs prefrontal functional connectivity, resulting in reduced global connectivity and impaired long-range coupling in parieto-temporal associative regions of the default mode network. We corroborate these findings in a mouse model of 16p11.2 deletion (Horev *et al.*, 2011), in which we observed similarly reduced long-range prefrontal connectivity, as well as thalamo-prefrontal miswiring and reduced low-frequency neuronal synchronization. Our results in mouse and human suggest that deletion in 16p11.2 may lead to impaired cognition and ASD-like symptoms via dysregulation of long-range prefrontal functional synchronization.

Material and methods

Full-length experimental procedures can be found in the online Supplementary material.

Ethical statement

All study procedures were approved by the institutional review board at the involved medical centres and are in accordance with the ethical standards of the Declaration of Helsinki of 1975, as revised in 2008. Animal studies were conducted in accordance with the Italian Law (DL 26/2014, EU 63/2010, Ministero della Sanità, Roma) and the recommendations in the Guide for the Care and Use of Laboratory Animals of the National Institutes of Health. Animal research protocols were also reviewed and consented to by the animal care committee. All surgical procedures were performed under deep anaesthesia.

Human resting state functional MRI

RsfMRI mapping focused on initially identified probands and their siblings with deletion at 16p11.2 as part of a multicentre investigation (Simons VIP Consortium, 2012). MRI was performed on 3 T Tim magnetic resonance scanners with repetition time = 3000 ms, echo time = 30 ms, 124 repetitions for a total scan time of 6 min 12 s. A final list of 19 paediatric deletion carriers (age 8–16 years; 10 males and nine females) and 28 paediatric control subjects (age 7–16 years; 16 males and 12 females) were included in the study. A breakdown of subject demographics is reported in Table 1 and Supplementary Table 1. Image preprocessing was based on previous studies of the ABIDE dataset (Di Martino *et al.*, 2014) and on the Preprocessed Connectomes Project. To control for motion contamination, we removed all frames whose frame-wise

Table 1 Demographics

	Paediatric controls	Paediatric 16p11.2 del carriers
Age (years)	12.49 ± 2.24	11.52 ± 2.53
Gender	16 M/12 F	10 M/9 F
NVIQ**	105 ± 12	93 ± 18
FSIQ**	106 ± 15	89 ± 18
SRS***	16 ± 11	74 ± 37

**P < 0.01, ***P < 0.001, t-test. FSIQ = full-scale IQ; NVIQ = non-verbal IQ.

displacement was larger than 0.5 mm (Power et al., 2012; Di Martino et al., 2014) and we only retained subjects in which >80% of rsfMRI volumes were retained. The number of scrubbed volumes and mean frame-wise displacement for each subject are reported in Supplementary Table 2. The whole preprocessing pipeline was implemented using the Configurable Pipeline for the Analysis of Connectomes (C-PAC v1.0.1a).

Network centrality was mapped as implemented in C-PAC (Di Martino et al., 2014). To map intergroup differences in connectivity we applied a multiple regression model [covariates: age, gender, group-centred non-verbal IQ, site, and mean frame-wise displacement] and used a t-test to assess the statistical significance of the regression coefficient corresponding to the group variable [$P < 0.05$, family-wise error corrected, with cluster-defining threshold of $t(40) > 2.01$, $P < 0.05$ as implemented in FSL]. We subsequently performed a seed-based analysis using a seed in the medial prefrontal area exhibiting significantly reduced centrality in the 16p11.2 deletion group (Fig. 1A), using a multiple regression model as above. Linear Discriminant Analysis (LDA) was performed using MASS library v7.3 (Venables and Ripley, 2002).

Mouse studies

Functional and structural MRI

RsfMRI experiments were performed on male adult 16p11.2$^{+/-}$ mice and wild-type littermates ($n = 12$ and $n = 11$, respectively) using halothane-induced sedation. Animal preparation has been recently described in greater detail (Ferrari et al., 2012; Sforazzini et al., 2014). Intergroup differences in functional connectivity were mapped using network centrality and seed-based mapping to recapitulate the approach applied to human imaging data (Liska et al., 2015, 2018). Diffusion-weighted MRI was carried out on the same subjects used for rsfMRI mapping in paraformaldehyde fixed specimens as previously described (Dodero et al., 2013). Brains were imaged inside intact skulls to avoid post-extraction deformations. Magnetic resonance tractography was carried out as previously described (Liska et al., 2018). To qualitatively compare white matter microstructural parameters in humans

and mice, we mapped fractional anisotropy using tract-based spatial statistics (TBSS) analysis, as implemented in FSL (Dodero et al., 2013).

In vivo electrophysiology

Experiments were performed on 16p11.2$^{+/-}$ and control littermates ($n = 6$, each group) as previously described (Zhan et al., 2014) using two electrodes placed in the prefrontal and retrosplenial cortex. Local field potential recordings were carried out under halothane sedation to reproduce the conditions of rsfMRI.

Retrograde viral tracing with rabies virus

Unpseudotyped recombinant SADΔG-mCherry rabies virus (RV) was produced as described in Osakada and Callaway (2013). Prefrontal rabies virus injections were carried out and quantified as previously described (Sforazzini et al., 2016) in adult male 16p11.2$^{+/-}$ and control 16p11.2$^{+/+}$ littermates ($n = 6$, each group).

Dendritic spine analysis

Experiments were performed on adult control and 16p11.2$^{+/-}$ mice ($n = 8$, each group). We quantified the density of dendritic spines in the anterior cingulate cortex and somatosensory cortex using the Golgi-Cox staining method as recently described (Martino et al., 2013).

Brain slice electrophysiology

Brain slice electrophysiology was carried out as recently described (Giorgi et al., 2017) on young adult 16p11.2$^{+/+}$ and 16p11.2$^{+/-}$ mice (12 weeks old, $n = 4$ per group). Whole-cell patch-clamp recordings were made on pyramidal neurons of the layer V of the prefrontal cortex. Spontaneous excitatory postsynaptic currents (sEPSCs) were recorded in the presence of 10 μM gabazine. For miniature EPSCs (mEPSCs), recordings were made also in the presence of 1 μM tetrodotoxin.

Electron microscopy

Conventional electron microscopy was carried out as described in Zhan et al. (2014), using adult 16p11.2$^{+/-}$ ($n = 4$) and control littermate ($n = 3$) mice.

Results

Reduced prefrontal connectivity in 16p11.2 deletion carriers

To investigate whether 16p11.2 deletion affects brain functional connectivity, we mapped rsfMRI connectivity in human children with 16p11.2 deletion and control subjects ($n = 19$, and $n = 28$, respectively; Simons VIP consortium,
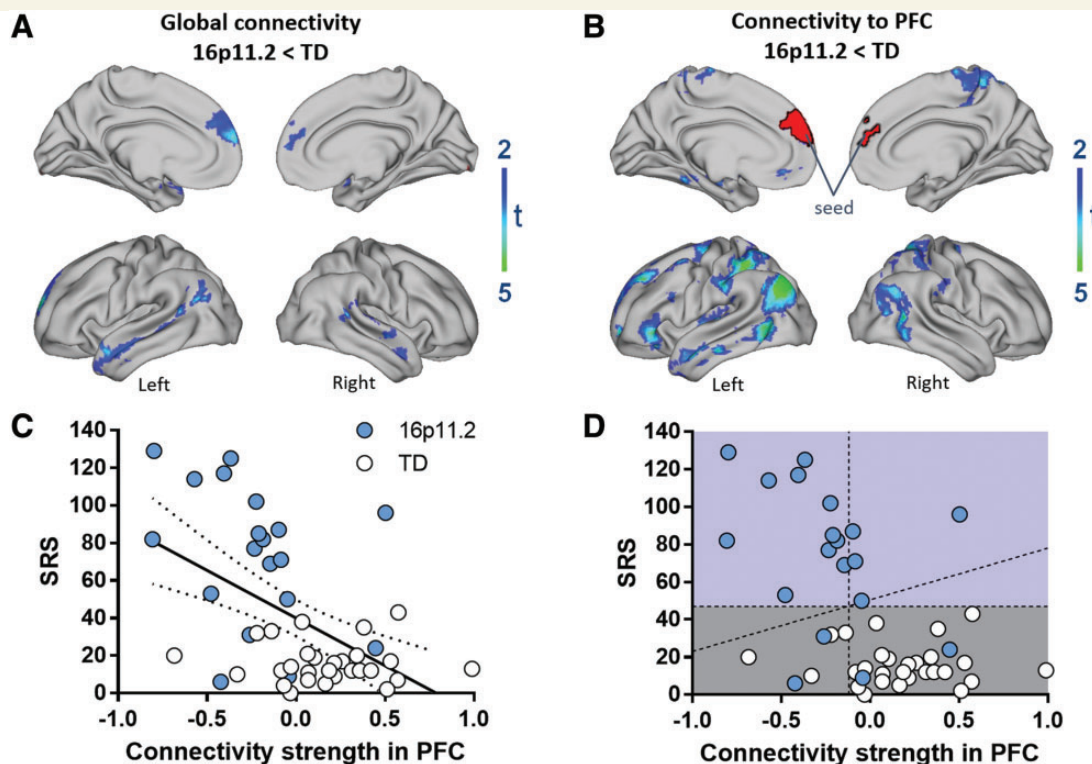
Figure 1 Reduced prefrontal connectivity in 16p11.2 deletion carriers. (**A**) Whole-brain voxel-wise mapping of intergroup differences in rsfMRI connectivity revealed reduced global connectivity in the medial PFC of 16p11.2 deletion carriers ($P < 0.05$, cluster-corrected) with respect to typically developing (TD) control subjects. Additional foci of reduced connectivity were located in temporal and parietal areas (superior and medial temporal gyrus, and temporal-parietal junctions). (**B**) Targets of the PFC underconnectivity, identified using a seed-based analysis. We used a seed region (shown in red) covering the whole PFC area exhibiting significant inter-group differences in **A**. Functional connectivity reductions were observed in the latero-temporal cortex, and inferior parietal lobule, as well as in the superior and inferior frontal cortex and paracentral gyrus of 16p11.2 deletion carriers ($P < 0.05$, cluster corrected). (**C**) PFC connectivity strength exhibited robust inverse correlation with SRS score ($r = -0.52$, $P < 0.001$). (**D**) Linear discrimination analysis of the predictive power of PFC connectivity and SRS score of CNV in individual subjects. SRS score and connectivity strength were assessed either alone (vertical and horizontal dashed line, respectively) or in combination (diagonal dashed line).

2012). In keeping with prior investigations in the same patient cohort (Owen et al., 2014), full-scale and non-verbal IQ were significantly lower, while social responsiveness score was higher in deletion carriers with respect to control subjects [$t(44) = 3.47$, $P = 0.001$; $t(45) = 2.83$, $P = 0.007$; $t(45) = 7.78$, $P < 0.001$, respectively, t-test]. Demographics and diagnosis are reported in Table 1 and Supplementary Table 1, respectively.

To obtain a spatially unbiased assessment of brain-wide functional connectivity, we mapped whole-brain global connectivity differences across the two cohorts. The metric used, also referred to as weighted degree centrality (Cole et al., 2010; Rubinov and Sporns, 2011), is a good predictor of higher socio-cognitive performance (Cole et al., 2012) and a sensitive marker of network dysfunction in brain connectopathies (Cole et al., 2011; Supekar et al., 2013; Di Martino et al., 2014; Cheng et al., 2015). Whole-brain voxel-wise mapping revealed reduced global connectivity in the medial prefrontal cortex (PFC) of 16p11.2 deletion carriers [Fig. 1A, $P < 0.05$, family-wise corrected with a cluster-defining threshold $t(40) > 2.01$]. We also observed foci of reduced connectivity in temporal and parietal areas involved in

socio-cognitive functioning, such as the superior and medial temporal gyrus, and temporal-parietal junctions (Fig. 1A).

To map the target regions underlying the identified connectivity reduction, we probed whole-brain functional connectivity using a seed region placed in the affected medial prefrontal area (Fig. 1B). We chose the PFC because of its key involvement in social cognition and higher cognitive functions (Blakemore, 2008; Cole et al., 2012; Grossmann, 2013), two domains that are impaired in 16p11.2 deletion carriers (Zufferey et al., 2012). This analysis revealed the presence of reduced long-range connectivity with the PFC in multiple areas of 16p11.2 deletion carriers (Fig. 1B). Prominent connectivity reductions were observed in the latero-temporal cortex, and inferior parietal lobule, two associative regions of the default mode network, as well as in the superior and inferior frontal cortex and paracentral gyrus [$P < 0.05$, family-wise corrected, with cluster-defining threshold of $t(40) > 2.01$]. A similar pattern of hypoconnectivity was obtained when non-verbal IQ was not used as covariate in the regression model (Supplementary Fig. 1). These findings reveal the presence of reduced long-range functional connectivity in the medial prefrontal cortex of human 16p11.2 deletion carriers.

PFC connectivity strength exhibited strong inverse correlation with social responsiveness scale (SRS) score (r = −0.52, P < 0.001, n = 47, Fig. 1C). To investigate the combined predictive power of SRS score and PFC connectivity strength on CNV status, we used a linear discriminant analysis (Fig. 1D). We found that PFC connectivity strength alone leads to a correct classification of CNV status in 24/28 of controls (specificity = 85.7%) and 13/19 deletion subjects (sensitivity = 68.4%), with an overall accuracy of 37/47 (78.7%). SRS scores *per se* exhibited higher predictive value, leading to a correct classification of 28/28 controls (specificity = 100%) and 15/19 deletion subjects (sensitivity = 78.9%) with an overall accuracy of 43/47 (91.5%). The combined use of PFC connectivity strength and SRS scores did not improve prediction of CNV status, leading to the same specificity, sensitivity and accuracy obtained with SRS score alone. PFC connectivity strength was also moderately correlated with full-scale IQ and non-verbal IQ (r = 0.47, P = 0.001, and r = 0.38, P = 0.009, respectively, n = 47, Supplementary Fig. 2).

Reduced prefrontal connectivity and neural synchronization in a mouse model of 16p11.2 deletion

To corroborate the human findings and bolster a role of 16p11.2 deletion in affecting prefrontal connectivity, we used rsfMRI to map functional connectivity in a mouse line harbouring a deletion in orthologous regions to human 16p11.2 (Horev *et al.*, 2011) under light sedation. The imaging approach used permits to probe large-scale network organization in rodents (Gozzi and Schwarz, 2016) and is highly sensitive to genetic and developmental modulation of macroscale connectivity (Sforazzini *et al.*, 2016; Liska *et al.*, 2018). Based on human findings we hypothesized that similar prefrontal long-range connectivity impairments could be identified in 16p11.2$^{+/-}$ mice. To test this hypothesis, we first mapped whole-brain global connectivity differences between 16p11.2 mutant mice and control littermates using the same connectivity metric used for human mapping (weighted degree centrality, Liska *et al.*, 2015). The approach revealed a focal reduction in global connectivity in the medial prefrontal cortex of 16p11.2$^{+/-}$ mutant mice [Fig. 2A, P < 0.05, cluster-defining threshold $t(21) > 2.08$], consistent with the global connectivity differences observed in human 16p11.2 deletion carriers. To probe the long-range substrates affected by the identified prefrontal hypoconnectivity, we next carried out seed-based mapping using a seed centred in the PFC. This analysis revealed a significant connectivity reduction in posterior parietal and retrosplenial cortices [Fig. 2B, P < 0.05, cluster-defining threshold $t(21) > 2.08$], two associative regions of the mouse default mode network involved in sensory integration (Robinson *et al.*, 2014; Gozzi and Schwarz, 2016; Whitlock, 2017). Foci of reduced connectivity were also observed in the

medial-dorsal thalamus. To further probe the presence of long-range functional coupling with the prefrontal cortex in 16p11.2 mutants, we carried out a seed-based quantification of prefrontal connectivity across midline cortical regions of the mouse brain. This analysis revealed a significant reduction in long-rage connectivity in 16p11.2$^{+/-}$ mice along the rostro-caudal axis of the cingulate and retrosplenial cortex [repeated measures two-way ANOVA, genotype-effect: $F(1,21) = 5.70$, P = 0.027, Fig. 2C and D]. Interhemispheric connectivity in subcortical or motor-sensory rsfMRI networks appeared to be otherwise preserved (Supplementary Fig. 3).

To corroborate a neural origin for the observed connectivity reduction, we carried out local field potential coherence measurements in a separate cohort of mice under the same experimental conditions used in our imaging studies. We probed the presence of long-range connectivity deficits by placing electrodes in the prefrontal and retrosplenial cortex, two regions characterized by reduced functional coupling in 16p11.2 mutants as assessed with rsfMRI. These measurements highlighted reduced long-range low-frequency local field potential coherence in 16p11.2$^{+/-}$ mice, resulting in a robust genotype × frequency interaction [$F(156,1560) = 2.29$, P < 0.001, Fig. 2E] and a reduction in the delta frequency power [t-test, $t(10) = 3.73$, P = 0.007, $q_{FDR} = 0.028$, Fig. 2F], a rhythmic activity that is strongly correlated with spontaneous functional MRI fluctuations (Lu *et al.*, 2007). These findings suggest that 16p11.2 deletion can reduce long-range prefrontal coupling via impaired low-frequency synchronization.

Importantly, we did not observe genotype-dependent differences in anaesthesia sensitivity as measured with arterial blood pressure mapping [t-test, $t(21) = 0.96$, P = 0.35; Supplementary Fig. 4] or amplitude of cortical blood oxygen level-dependent signal fluctuations [t-test, $t(21) = 0.16$, P = 0.87, Supplementary Fig. 4], two independent readouts linearly correlated with anaesthesia depth (Steffey *et al.*, 2003; Liu *et al.*, 2011). Minimal alveolar concentration, another measure of anaesthesia sensitivity, was also comparable across experimental groups ($1.31 \pm 0.08\%$ and $1.34 \pm 0.09\%$, respectively, P = 0.48, Kolmogorov-Smirnov test). These results argue against a confounding contribution of the anaesthetic to the observed connectivity impairments in 16p11.2$^{+/-}$ mice.

Altered thalamo-prefrontal wiring in 16p11.2$^{+/-}$ deletion mice

To probe a contribution of macroscopic white matter rearrangement to the observed functional hypoconnectivity, we carried out MRI tractography analysis of the corpus callosum, cingulum and anterior commissure, three major white matter tracts characterized by extensive cortico-cortical, antero-posterior extension. We found these white matter bundles to be largely typical in mutant and control mice (Fig. 3A). Fibre streamline quantifications did not
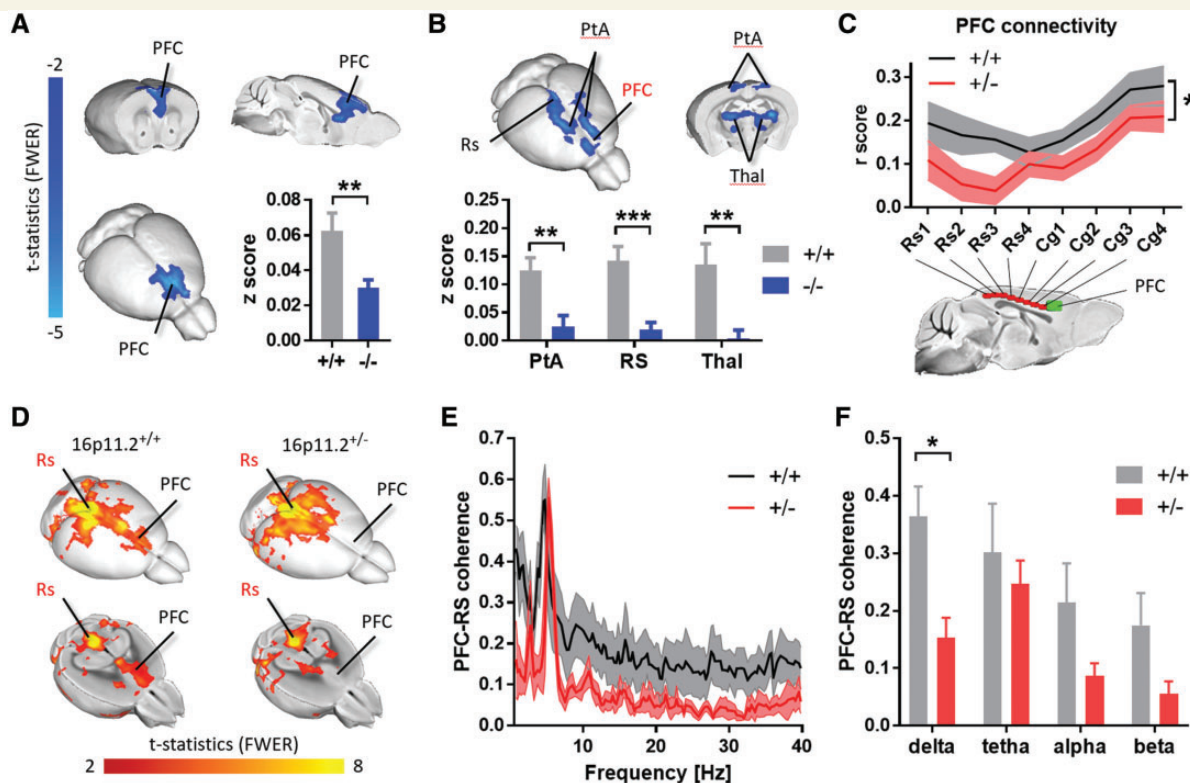
Figure 2 Reduced prefrontal connectivity and low-frequency synchronization in 16p11.2$^{+/-}$ mice. (**A**) Whole-brain voxel-wise mapping of global connectivity revealed reduced functional connectivity in the medial PFC of 16p11.2$^{+/-}$ mutant mice compared to control littermates ($P < 0.05$, cluster-corrected). (**B**) Seed-based mapping of the PFC (green seed, **C**) revealed foci of reduced rsfMRI connectivity in parieto-temporal areas (PtA), retrosplenial cortex (Rs) and thalamus (Thal) of 16p11.2$^{+/-}$ mutants ($P < 0.05$, cluster-corrected). *Inset* plots show a quantification of the effect size in the regions affected [*$P < 0.05$, **$P < 0.01$, ***$P < 0.001$, Student *t*-test, means $\pm$ standard error of the mean (SEM)]. (**C**) Connectivity profile between a series of midline seeds (Cg = cingulate cortex) and the PFC (green) (*$P < 0.05$, two-way repeated measures ANOVA, mean $\pm$ SEM). (**D**) Seed correlation maps in control and 16p11.2 mutants highlighting reduced extension of long-range connectivity between the retrosplenial and PFCs (seed Rs3, $P < 0.05$ FWE cluster-corrected). (**E** and **F**) Local field potential (LFP) coherence measurements highlighted a reduction in long-range local field potential coherence in 16p11.2$^{+/-}$ mice, resulting in a robust genotype $\times$ frequency interaction [$F(191,1910) = 2.487$, $P < 0.001$, **E**, means $\pm$ SEM) and a significant reduction in delta frequency range (*$P < 0.05$, **F**, means $\pm$ SEM).

reveal any genotype-dependent differences in the number of streamlines [cingulum: $t(23) = 1.51$, $P = 0.14$; corpus callosum: $t(23) = 1.45$, $P = 0.16$; Supplementary Fig. 5]. These results rule out a contribution of gross macroscale white matter alterations to the observed functional hypoconnectivity.

To examine the presence of finer-scale wiring alterations undetectable by tractography, we carried out monosynaptic retrograde tracing of the left prefrontal cortex in 16p1.2$^{+/-}$ mice. Besides being a key cortical substrate affected by 16p11.2 deletion, this region also receives widespread innervation by the thalamus (Hoover and Vertes, 2007; Liska *et al.*, 2018), an anatomical substrate involved in the generation of delta activity (McCormick and Pape, 1990). This characteristic offers the opportunity to establish a putative link between mesoscale connectional alterations and the observed reduction in functional connectivity. Quantification of the relative fraction of labelled cells revealed the presence increased projection frequency in the mediodorsal thalamus of 16p1.2$^{+/-}$ mice

$[t(10) = 4.55$, $P = 0.001$, FDR corrected, Fig. 3B and C], a region exhibiting reduced rsfMRI synchronization with the PFC (Fig. 2B). No genotype-dependent difference in the frequency of prefrontal projecting neurons was observed in any of the other cortical or subcortical regions examined (Fig. 3C).

Because altered long-range projection input may affect synaptic input and dendritic spine density in target regions (Glausier and Lewis, 2013), we also quantified dendritic spine density in cortical layers 2/3 in dysfunctional (PFC) and unaffected (somatosensory) cortical areas of 16p11.2$^{+/-}$ mice. Interestingly, we observed a significant reduction in dendritic spine density in the PFC, but not in the somatosensory cortex of 16p11.2$^{+/-}$ mice $[t(15) = 5.11$, $P = 0.00012$, FDR corrected, Supplementary Fig. 6A]. These results corroborate the regional specificity of the observed functional impairments, and suggest a possible contribution of synaptic deficits to the prefrontal impairment observed in 16p11.2 deletion. Whole-cell patch clamp electrophysiological recordings in prefrontal
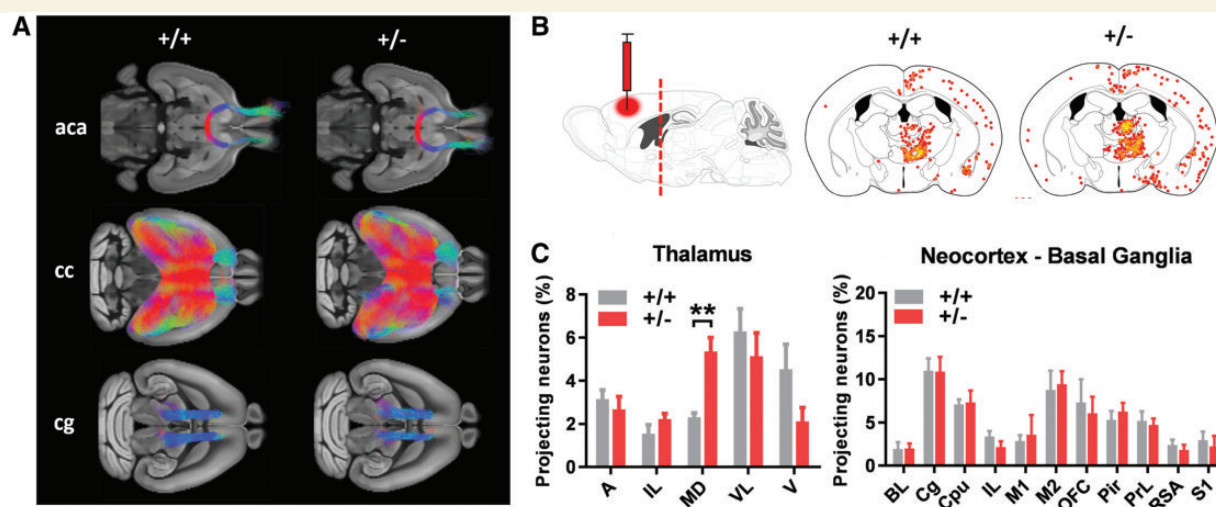
Figure 3 Altered thalamo-frontal wiring in 16p11.2$^{+/-}$ mice. (**A**) Anterior commissure, corpus callosum and cingulum tracts virtually dissected in two representative mice (16p11.2$^{+/+}$ *top*, 16p11.2$^{+/-}$ *bottom*). We did not observe any genotype-dependent differences in the macroscale organization of these major white matter tracts (Supplementary Fig. 5). (**B**) Regional distribution of retrogradely-labelled cells in the thalamus of control (16p11.2$^{+/+}$) and 16p11.2$^{+/-}$ mutant mice after injection of recombinant rabies virus in the prefrontal cortex. (**C**) Quantification of the frequency of retrogradely-labelled cells in neocortical areas and subthalamic regions revealed focally increased projection frequency in the mediodorsal thalamus (MD) of 16p11.2$^{+/-}$ mice (**$P < 0.01$, FDR corrected, means ± SEM). A = anterior thalamus; BL = basolateral amygdala; Cg = cingulate cortex; Cpu = caudate putamen; IL = infralimbic cortex; IL = intralaminar thalamus; M1 = primary motor cortex; M2 = secondary motor cortex; MD = mediodorsal thalamus; OFC = orbitofrontal cortex; Pir = piriform cortex; PrL = prelimbic cortex; RSA = retrosplenial cortex; S1 = somatosensory cortex; V = ventral thalamus; VL = ventrolateral thalamus.

pyramidal neurons of 16p11.2$^{+/-}$ mice did not reveal genotype-dependent differences in spontaneous and miniature EPSCs (Supplementary Fig. 6B–E).

Widespread white matter microstructure alterations in 16p11.2$^{+/-}$ mice

We finally examined the presence of microscale white matter structural abnormalities in 16p11.2$^{+/-}$ mutants via magnetic resonance-based measurements of fractional anisotropy, a marker of microstructural integrity that has been recently described to be altered in the same patient cohort examined here (Owen *et al.*, 2014; Chang *et al.*, 2016). In keeping with human findings, we found widespread increase in fractional anisotropy in major white matter tracts of 16p11.2$^{+/-}$ mice [$P < 0.05$, corrected with threshold-free cluster enhancement, Fig. 4A and C; $t(23) = 2.48$, $P = 0.021$], suggesting that 16p11.2 deletion similarly affects white matter microstructure in humans and rodents. By using electron microscopy, we identified increased axonal diameter in callosal fibres as a plausible cellular correlate of these alterations (Fig. 4B). Specifically, we found callosal neurons to have thicker myelin [$t(446) = 2.7$, $P = 0.007$, Fig. 4C], larger diameter [$t(348) = 2.498$, $P = 0.012$, Fig. 4C] and a higher g ratio [$t(446) = 2.58$, $P = 0.010$, Fig. 4C] in 16p11.2$^{+/-}$ mice with respect to control littermates. In contrast with the more focal functional impairments observed in 16p11.2 deletion carriers and in the mouse model, the microstructural

alteration appeared to be widespread and as such is unlikely to represent a direct correlate of the observed functional hypoconnectivity.

Discussion

Here we show that 16p11.2 deletion results in reduced prefrontal connectivity and impaired long-range functional coupling with temporal-parietal regions. We also document that a mouse line with the same genetic deficiency exhibits similarly diminished reduced prefrontal connectivity, together with thalamo-prefrontal miswiring and reduced long-range low-frequency neural synchronization. These findings establish a link between a common ASD-associated CNV and impaired macroscale connectivity, suggesting that 16p11.2 deletion can predispose to neurodevelopmental disorders and impaired socio-cognitive function via a dysregulation of long-range prefrontal synchronization. The paradigm used here—in which functional neuroimaging across species is used to explore the functional consequences of a known disease-associated variant in a highly focused manner—is likely to be of widespread utility in the elucidation of the mechanisms underlying the functional disconnectivity associated with disorders of human cognition and development.

The observed connectivity impairments add to an increasing body of experimental work pointing at the presence of aberrant functional synchronization in ASD and severe developmental disorders. While largely heterogeneous in its manifestation, brain-wide functional connectivity has been
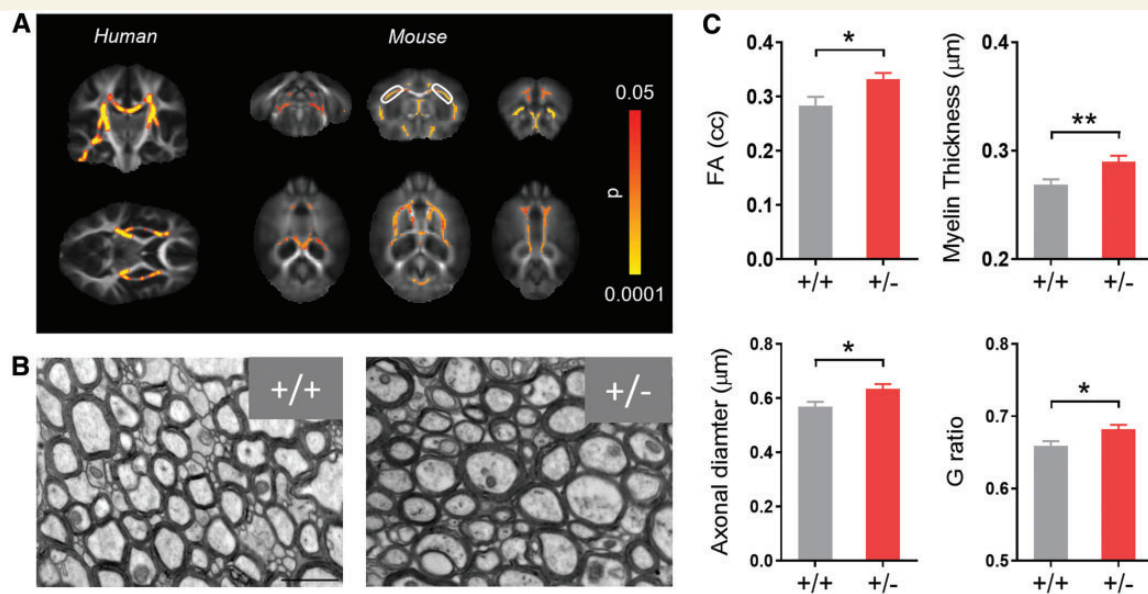
Figure 4 Comparable white matter microstructural abnormalities in human 16p11.2 deletion carriers and 16p11.2$^{+/-}$ mice.
(**A**) White matter regions exhibiting significantly increased fractional anisotropy (FA) in human deletion carriers (*left*, modified from Owen *et al.*
2014, with permission). Voxelwise mapping of FA in mouse revealed analogous increases in 16p11.2$^{+/-}$ mutants (*right*). (**B**) Transmission electron
micrographs of corpus callosum cross-sections from control (+/+) and 16p11.2$^{+/-}$ (+/−) mice. Scale bar = 1 μm; original magnification
×25 000. (**C**) Quantification of fractional anisotropy, mean thickness, axonal diameter and G-ratio in callosal neurons (*$P < 0.05$, **$P < 0.01$,
means ± SEM).

reported to be largely disrupted in autistic patients (Vasa
et al., 2016; Hull *et al.*, 2017). Our results underscore a
contribution of impaired long-range functional synchron-
ization as a key predisposing factor of cognitive and
social impairments associated with 16p11.2 deletion. The
involvement of prefrontal areas as well as associative re-
gions of the default mode network is consistent with prior
rsfMRI studies, which have reported this network as being
particularly vulnerable in ASD (Di Martino *et al.*, 2014;
Washington *et al.*, 2014). As brain maturation is reflected
in strengthening of long-range cortical-cortical connectivity
(Dosenbach *et al.*, 2010), the observed functional impair-
ments could be indicative of a delayed or immature
connectivity between higher-order integrative regions.
According to this view, the involvement of prefrontal re-
gions may reflect the especially slow maturation of these
substrates, a process that continues up to adulthood
(Sowell *et al.*, 1999). The reduced connectivity observed
in temporal-parietal areas and in associative regions of
the default mode network is also equally noteworthy,
owing to the implication of these areas in socio-cognitive
functions that are impaired in 16p11.2 deletion carriers and
ASD patients (Bernhardt *et al.*, 2014; Cheng *et al.*, 2015;
Hanson *et al.*, 2015). The fact that the observed connec-
tional impairments are not strictly dependent on a specific
diagnosis suggests that this CNV mediates risk by modulat-
ing the continuum of normal brain function, as would be
expected for intermediate phenotypes related to cogni-
tion and behaviour (Scott-Van Zeeland *et al.*, 2010;
Rudie *et al.*, 2012).

The presence of reduced prefrontal connectivity in a
mouse line recapitulating human 16p11.2 deletion under-
scores the involvement of prefrontal integrative regions as a
key macroscale substrate of this genetic deficiency, and
offers the possibility of generating hypotheses about pos-
sible neural mechanisms underlying this impairment. A
macroscale investigation of white matter connectivity
using diffusion tensor imaging ruled out the presence of
major structural rearrangements in 16p11.2 mutants.
However, functional connectivity alterations are rarely a
direct proxy of underlying white matter reorganization
(Anagnostou and Taylor, 2011), and remarkable examples
of dissociation between macroscopic anatomical organiza-
tion and functional connectivity have been described in
humans (Tyszka *et al.*, 2011; Paul *et al.*, 2014). The obser-
vation of increased thalamo-frontal wiring and functional
dysconnectivity in 16p11.2$^{+/-}$ mutants points at the in-
volvement of mesoscopic alterations in long-range project-
ing populations as a putative driver of this endophenotype,
possibly the result of abnormal synaptic refinement or cir-
cuit maturation during early development (Zhan *et al.*,
2014; Riccomagno and Kolodkin, 2015). As 16p11.2$^{+/-}$
mice exhibit altered cortical progenitor proliferation and
increased density of cortico-thalamic projecting neurons
(Pucilowska *et al.*, 2015), this abnormality could reflect
defective cortical feedback, leading to compromised feed-
forward refinement of thalamo-prefrontal projections
(Thompson *et al.*, 2016) and increased synaptic multipli-
city, a neural phenotype associated with autism-like behav-
iour and reduced functional connectivity in the mouse

(Zhan *et al.*, 2014). The observation of impaired delta rhythms in 16p11.2 mutant mice is broadly consistent with this hypothesis, given the key involvement of thalamic relay neurons in the generation of delta activity (McCormick and Pape, 1990). The presence of altered spine density in prefrontal but not motor-sensory areas of $16p11.2^{+/-}$ mice corroborates the regional specificity of the network alterations observed, and provides additional mechanistic clues to the observed functional impairments. Because thalamo-cortical inputs represent a limited proportion of all glutamatergic synapses in the cortex (Peters, 2002), a decreased spine density may reflect maturational deficits affecting microscale cortico-cortical connectivity. A number of additional neurophysiological mechanisms could also play a role in the generation of neural desynchronization and reduced functional connectivity, including altered inhibitory/excitatory activity, a feature associated with several autism-related mutations (Marín, 2012) and resulting in inefficient long-range synchronization (Cardin *et al.*, 2009). By contrast, the widespread increase in white matter fractional anisotropy observed in $16p11.2^{+/-}$ mice represents an unlikely correlate of the observed network alterations, given its widespread distribution and lack of pathway specificity. The correspondence with analogous fractional anisotropy mapping in human 16p11.2 carriers (Owen *et al.*, 2014; Chang *et al.*, 2016) is, however, of interest *per se,* as it represents an intrinsic corroboration of the translational validity of the mouse model employed as far as white matter microstructure is concerned.

Despite the considerable evolutionary distance between rodents and humans, our direct comparison of orthologous 16p11.2 mutations revealed broadly similar prefrontal functional hypoconnectivity across-species, as well as reduced long-range rsfMRI coupling between prefrontal and long-range associative cortical areas. Discrepancies in the location of these effects were also noted, such as the observation of reduced retrosplenial and thalamic connectivity in mouse but not human 16p11.2 deletion carriers, and a larger involvement of latero-cortical regions in the clinical cohort. Evolutionary differences in the organization and extension of prefrontal and associative cortices can plausibly account for some of these discrepancies. Postero-parietal associative areas in rodents are disproportionately smaller than their primate counterparts (Whitlock, 2017), and rodents lack regions cyto-architecturally homologous to the human ventral or dorsolateral PFC, or the precuneus (Vogt and Paxinos, 2014; Carlén, 2017). These divergences are consistent with a more focal involvement of parieto-cortical areas in 16p11.2 mutant mice. Moreover, thalamo-frontal functional coupling in rodents is considerably stronger than in humans, as documented by the involvement of thalamic areas as core constituents of the rodent, but not human, default mode network (Gozzi and Schwarz, 2016; Cunningham *et al.*, 2017). Stronger thalamo-frontal synchronization in rodents may explain the different thalamic involvement observed in this study. By contrast, the lack of retrosplenial/precuneal

hypoconnectivity in human 16p11.2 deletion carriers cannot be straightforwardly accounted for in evolutionary terms, given the comparably strong coupling of these areas with prefrontal cortex in both species (Gozzi and Schwarz, 2016). However, cross-species differences in the topology, organization and connectivity of these areas exist, the most notable of which being an antero-posterior shift of these areas as high-centrality integrative 'network hubs', ranging from prefrontal substrates in rodent to precuneal and posterior midline regions in primate and human (Liska *et al.*, 2015). Finally, additional experimental (e.g. anaesthesia) and biological differences could contribute to the observed spatial discrepancies, including species-specific neuroadaptive or compensatory mechanisms secondary to 16p11.2 deletion, and the impossibility to fully and closely replicate experimental conditions across species as a result of technical or procedural constraints.

Using the same imaging paradigm employed here, we recently identified impaired prefrontal connectivity in mice harbouring mutations in autism-risk gene *Cntnap2* (Liska *et al.*, 2018), an effect that recapitulates analogous observations in human carriers of *CNTNAP2* polymorphisms (Scott-Van Zeeland *et al.*, 2010). Prefrontal reductions in connectivity have also been reported in other mouse lines recapitulating autism-associated risk factors such as callosal agenesis (Sforazzini *et al.*, 2016), or genetic mutations involving cell adhesion or synaptic scaffolding genes (Michetti *et al.*, 2017; Pagani *et al.*, 2017). These correspondences suggest that impaired prefrontal connectivity could underlie core cognitive and behavioural deficits shared by multiple autism-associated genetic aetiologies. Prefrontal aberrancies are, however, unlikely to represent a single unifying mechanism in autism, as opposing functional alterations have been reported in human studies (Hull *et al.*, 2017) and are also emerging in mouse imaging studies. For example, mice harbouring a mutation in autism-associated gene *Chd8* show increased functional connectivity in hippocampal and sensory regions (Suetterlin *et al.*, 2018). By extending this investigational paradigm to multiple ASD-related risk factors it will be possible to identify shared connectional signatures, and formally probe a contribution of genetic variability to the heterogeneous expression of functional dysconnectivity in patient populations.

From a methodological standpoint, our rsfMRI results are bolstered by their recapitulation in two species, but also by a link to clinical symptoms revealing more severe socio-cognitive deficits in children exhibiting greater reductions in prefrontal functional connectivity. A confounding contribution of motion-related artefacts (Power *et al.*, 2015) to our human findings is highly unlikely, because we found overall motion to be comparable across groups, we used the 'scrubbing' method at a motion threshold used for rsfMRI connectivity assessment in prominent clinical ASD databases (0.5 mm; Di Martino *et al.*, 2014; Falahpour *et al.*, 2016; Balsters *et al.*, 2018) and we also conservatively analysed only subjects in which censoring permitted to retain >80% of the original time series. We also regressed mean framewise displacement as a

covariate of no interest. Although stricter motion censoring has been proposed (e.g. 0.2 mm; Supekar *et al.*, 2013) this threshold did not permit us to retain a sufficient number of subjects for statistical mapping in this study. We therefore resorted to replicate these measurements in the mouse, in which the use of sedation and mechanical ventilation results in negligible motion contamination (Ferrari *et al.*, 2012). Collectively, our findings strongly argue against a confounding role of motion in the impaired prefrontal connectivity observed in 16p11.2 deletion carriers.

In conclusion, here we document that 16p11.2 deletion leads to impaired prefrontal functional connectivity in mouse and human, an effect associated with aberrant fronto-thalamic wiring and long-range neural desynchronization. Our findings suggest that 16p11.2 deletion may predispose to neurodevelopmental disorders and autism through selective dysregulation of connectivity in integrative prefrontal areas, and provide a translational model for investigating connectional perturbations associated with syndromic developmental disorders.

Supplementary material

Supplementary material is available at *Brain* online.

References

Anagnostou E, Taylor M. Review of neuroimaging in autism spectrum disorders: what have we learned and where we go from here. Mol Autism 2011; 2: 4.

Balsters JH, Mantini D, Wenderoth N. Connectivity-based parcellation reveals distinct cortico-striatal connectivity fingerprints in autism spectrum disorder. Neuroimage 2018; 170: 412–23.

Bernhardt BC, Valk SL, Silani G, Bird G, Frith U, Singer T. Selective disruption of sociocognitive structural brain networks in autism and alexithymia. Cereb Cortex 2014; 24: 3258–67.

Blakemore SJ. The social brain in adolescence. Nat Rev Neurosci 2008; 9: 267–77.

Blumenthal I, Ragavendran A, Erdin S, Klei L, Sugathan A, Guide Jolene R, et al. Transcriptional consequences of 16p11.2 deletion and duplication in mouse cortex and multiplex autism families. Am J Hum Genet 2014; 94: 870–83.

Cardin JA, Carlén M, Meletis K, Knoblich U, Zhang F, Deisseroth K, et al. Driving fast-spiking cells induces gamma rhythm and controls sensory responses. Nature 2009; 459: 663–7.

Carlén M. What constitutes the prefrontal cortex? Science 2017; 358: 478–82.

Chang YS, Owen JP, Pojman NJ, Thieu T, Bukshpun P, Wakahiro ML, et al. Reciprocal white matter alterations due to 16p11. 2 chromosomal deletions versus duplications. Hum Brain Mapp 2016; 37: 2833–48.

Chen JA, Penaagarikano O, Belgard TG, Swarup V, Geschwind DH. The emerging picture of autism spectrum disorder: genetics and pathology. Ann Rev Pathol 2015; 10: 111–44.

Cheng W, Rolls ET, Gu H, Zhang J, Feng J. Autism: reduced connectivity between cortical areas involved in face expression, theory of mind, and the sense of self. Brain 2015; 138: 1382–93.

Cole MW, Anticevic A, Repovs G, Barch D. Variable global dysconnectivity and individual differences in Schizophrenia. Biol Psychiatry 2011; 70: 43–50.

Cole MW, Pathak S, Schneider W. Identifying the brain's most globally connected regions. Neuroimage 2010; 49: 3132–48.

Cole MW, Yarkoni T, Repovš G, Anticevic A, Braver TS. Global connectivity of prefrontal cortex predicts cognitive control and intelligence. J Neurosci 2012; 32: 8988–99.

Cunningham SI, Tomasi D, Volkow ND. Structural and functional connectivity of the precuneus and thalamus to the default mode network. Hum Brain Mapp 2017; 38: 938–56.

de la Torre-Ubieta L, Won H, Stein JL, Geschwind DH. Advancing the understanding of autism disease mechanisms through genetics. Nat Med 2016; 22: 345–61.

Di Martino A, Yan CG, Li Q, Denio E, Castellanos FX, Alaerts K, et al. The autism brain imaging data exchange: towards a large-scale evaluation of the intrinsic brain architecture in autism. Mol Psychiatry 2014; 19: 659–67.

Dodero L, Damiano M, Galbusera A, Bifone A, Tsaftsaris SA, Scattoni ML, et al. Neuroimaging evidence of major morpho-anatomical and functional abnormalities in the BTBR T + TF/J mouse model of autism. PLoS One 2013; 8: e76655.

Dosenbach NUF, Nardos B, Cohen AL, Fair DA, Power JD, Church JA, et al. Prediction of individual brain maturity using fMRI. Science 2010; 329: 1358–61.

Falahpour M, Thompson WK, Abbott AE, Jahedi A, Mulvey ME, Datko M, et al. Underconnected, but not broken? Dynamic functional connectivity MRI shows underconnectivity in autism is linked to increased intra-individual variability across time. Brain Connect 2016; 6: 403–14.

Ferrari L, Turrini G, Crestan V, Bertani S, Cristofori P, Bifone A, et al. A robust experimental protocol for pharmacological fMRI in rats and mice. J Neurosci Methods 2012; 204: 9–18.

Giorgi A, Migliarini S, Galbusera A, Maddaloni G, Mereu M, Margiani G, et al. Brainwide mapping of endogenous serotonergic transmission via chemogenetic-fMRI. Cell Rep 2017; 21: 910–18.

Glausier JR, Lewis DA. Dendritic spine pathology in schizophrenia. Neuroscience 2013; 251: 90–107.

Golzio C, Willer J, Talkowski ME, Oh EC, Taniguchi Y, Jacquemont S, et al. KCTD13 is a major driver of mirrored neuroanatomical phenotypes of the 16p11.2 copy number variant. Nature 2012; 485: 363–7.

Gozzi A, Schwarz AJ. Large-scale functional connectivity networks in the rodent brain. Neuroimage 2016; 127: 496–509.

Grossmann T. The role of medial prefrontal cortex in early social cognition. Front Hum Neurosci 2013; 7: 340.

Hanson E, Bernier R, Porche K, Jackson FI, Goin-Kochel RP, Snyder LG, et al. The cognitive and behavioral phenotype of the 16p11. 2

deletion in a clinically ascertained population. Biol Psychiatry 2015; 77: 785–93.

Hoover W, Vertes R. Anatomical analysis of afferent projections to the medial prefrontal cortex in the rat. Brain Struct Funct 2007; 212: 149–79.

Horev G, Ellegood J, Lerch JP, Son YEE, Muthuswamy L, Vogel H, et al. Dosage-dependent phenotypes in models of 16p11.2 lesions found in autism. Proc Natl Acad Sci USA 2011; 108: 17076–81.

Hull JV, Jacokes ZJ, Torgerson CM, Irimia A, Van Horn JD. Resting-state functional connectivity in autism spectrum disorders: a review. Front Psychiatry 2017; 7: 205.

Kumar RA, KaraMohamed S, Sudi J, Conrad DF, Brune C, Badner JA, et al. Recurrent 16p11.2 microdeletions in autism. Hum Mol Genet 2008; 17: 628–38.

Liska A, Bertero A, Gomolka R, Sabbioni M, Galbusera A, Barsotti N, et al. Homozygous loss of autism-risk gene CNTNAP2 results in reduced local and long-range prefrontal functional connectivity. Cereb Cortex 2018; 28: 1141–53.

Liska A, Galbusera A, Schwarz AJ, Gozzi A. Functional connectivity hubs of the mouse brain. Neuroimage 2015; 115: 281–91.

Liu X, Zhu XH, Zhang Y, Chen W. Neural origin of spontaneous hemodynamic fluctuations in rats under burst-suppression anesthesia condition. Cereb Cortex 2011; 21: 374–84.

Lu H, Zuo Y, Gu H, Waltz JA, Zhan W, Scholl CA, et al. Synchronized delta oscillations correlate with the resting-state functional MRI signal. Proc Natl Acad Sci USA 2007; 104: 18265–9.

Maillard AM, Ruef A, Pizzagalli F, Migliavacca E, Hippolyte L, Adaszewski S, et al. The 16p11.2 locus modulates brain structures common to autism, schizophrenia and obesity. Mol Psychiatry 2015; 20: 140–7.

Malhotra D, Sebat J. CNVs: harbingers of a rare variant revolution in psychiatric genetics. Cell 2012; 148: 1223–41.

Marín O. Interneuron dysfunction in psychiatric disorders. Nat Rev Neurosci 2012; 13: 107–20.

Martino A, Ettorre M, Musilli M, Lorenzetto E, Buffelli M, Diana G. Rho GTPase-dependent plasticity of dendritic spines in the adult brain. Front Cell Neurosci 2013; 7: 62.

McCormick A, Pape HC. Properties of a hyperpolarization-activated cation current and its role in rhythmic oscillation in thalamic relay neurones. J Physiol 1990; 431: 291–318.

Michetti C, Caruso A, Pagani M, Sabbioni M, Medrihan L, David G, et al. The knockout of synapsin II in mice impairs social behavior and functional connectivity generating an ASD-like phenotype. Cereb Cortex 2017; 27: 5014–23.

Osakada F, Callaway EM. Design and generation of recombinant rabies virus vectors. Nat Protoc 2013; 8: 1583–601.

Owen JP, Chang YS, Pojman NJ, Bukshpun P, Wakahiro MLJ, Marco EJ, et al. Aberrant white matter microstructure in children with 16p11.2 deletions. J Neurosci 2014; 34: 6214–23.

Pagani M, Liska A, Galbusera A, Gozzi A. Altered prefrontal functional connectivity and anatomy in mice lacking autism-associated gene Shank3. Society for Neuroscience Annual Meeting, 2017. Washington: Society for Neuroscience; 2017.

Paul LK, Corsello C, Kennedy DP, Adolphs R. Agenesis of the corpus callosum and autism: a comprehensive comparison. Brain 2014; 137: 1813–29.

Peters A. Examining neocortical circuits: some background and facts. J Neurocytol 2002; 31: 183–93.

Power JD, Barnes KA, Snyder AZ, Schlaggar BL, Petersen SE. Spurious but systematic correlations in functional connectivity MRI networks arise from subject motion. Neuroimage 2012; 59: 2142–54.

Power JD, Schlaggar BL, Petersen SE. Recent progress and outstanding issues in motion correction in resting state fMRI. Neuroimage 2015; 105: 536–51.

Pucilowska J, Vithayathil J, Tavares EJ, Kelly C, Karlo JC, Landreth GE. The 16p11.2 deletion mouse model of autism exhibits altered cortical progenitor proliferation and brain cytoarchitecture linked to the ERK MAPK pathway. J Neurosci 2015; 35: 3190–200.

Qureshi AY, Mueller S, Snyder AZ, Mukherjee P, Berman JI, Roberts TP. Opposing brain differences in 16p11.2 deletion and duplication carriers. J Neurosci 2014; 34: 11199–211.

Riccomagno MM, Kolodkin AL. Sculpting neural circuits by axon and dendrite pruning. Annu Rev Cell Dev Biol 2015; 31: 779–805.

Robinson S, Todd TP, Pasternak AR, Luikart BW, Skelton PD, Urban DJ, et al. Chemogenetic silencing of neurons in retrosplenial cortex disrupts sensory preconditioning. J Neurosci 2014; 34: 10982–8.

Rubinov M, Sporns O. Weight-conserving characterization of complex functional brain networks. Neuroimage 2011; 56: 2068–79.

Rudie JD, Hernandez LM, Brown JA, Beck-Pancer D, Colich NL, Gorrindo P, et al. Autism-associated promoter variant in MET impacts functional and structural brain networks. Neuron 2012; 75: 904–15.

Scott-Van Zeeland AA, Abrahams BS, Alvarez-Retuerto AI, Sonnenblick LI, Rudie JD, Ghahremani D, et al. Altered functional connectivity in frontal lobe circuits is associated with variation in the autism risk gene CNTNAP2. Sci Transl Med 2010; 2: 56ra80.

Sforazzini F, Bertero A, Dodero L, David G, Galbusera A, Scattoni M, et al. Altered functional connectivity networks in acallosal and socially impaired BTBR mice. Brain Struct Funct 2016; 221: 941–54.

Sforazzini F, Schwarz AJ, Galbusera A, Bifone A, Gozzi A. Distributed BOLD and CBV-weighted resting-state networks in the mouse brain. Neuroimage 2014; 87: 403–15.

Simons VIP Consortium. Simons Variation in Individuals Project (Simons VIP): a genetics-first approach to studying autism spectrum and related neurodevelopmental disorders. Neuron 2012; 73: 1063–7.

Sowell ER, Thompson PM, Holmes CJ, Jernigan TL, Toga AW. In vivo evidence for post-adolescent brain maturation in frontal and striatal regions. Nat Neurosci 1999; 2: 859–61.

Steffey MA, Brosnan RJ, Steffey EP. Assessment of halothane and sevoflurane anesthesia in spontaneously breathing rats. Am J Vet Res 2003; 64: 470–4.

Suetterlin P, Hurley S, Mohan C, Riegman KLH, Pagani M, Caruso A, et al. Altered neocortical gene expression, brain overgrowth and functional over-connectivity in Chd8 haploinsufficient mice. Cereb Cortex 2018; doi: 10.1093/cercor/bhy058.

Supekar K, Uddin LQ, Khouzam A, Phillips J, Gaillard WD, Kenworthy LE, et al. Brain hyperconnectivity in children with autism and its links to social deficits. Cell Rep 2013; 5: 738–47.

Thompson AD, Picard N, Min L, Fagiolini M, Chen C. Cortical feedback regulates feedforward retinogeniculate refinement. Neuron 2016; 91: 1021–33.

Tick B, Bolton P, Happé F, Rutter M, Rijsdijk F. Heritability of autism spectrum disorders: a meta-analysis of twin studies. J Child Psychol Psychiatry 2016; 57: 585–95.

Tyszka JM, Kennedy DP, Adolphs R, Paul LK. Intact bilateral resting-state networks in the absence of the corpus callosum. J Neurosci 2011; 31: 15154–62.

Vasa RA, Mostofsky SH, Ewen JB. The disrupted connectivity hypothesis of autism spectrum disorders: time for the next phase in research. Biol Psychiatry Cogn Neurosci Neuroimaging 2016; 1: 245–52.

Venables WN, Ripley BD. Modern applied statistics with S. 4th edn., New York: Springer; 2002.

Vogt B, Paxinos G. Cytoarchitecture of mouse and rat cingulate cortex with human homologies. Brain Struct Funct 2014; 219: 185–92.

Washington SD, Gordon EM, Brar J, Warburton S, Sawyer AT, Wolfe A, et al. Dysmaturation of the default mode network in autism. Hum Brain Mapp 2014; 35: 1284–96.

Whitlock JR. Posterior parietal cortex. Curr Biol 2017; 27: R691–5.

Zhan Y, Paolicelli R, Sforazzini F, Weinhard L, Bolasco G, Pagani F, et al. Deficient neuron-microglia signaling results in impaired functional brain connectivity and social behavior. Nat Neurosci 2014; 17: 400–6.

Zufferey F, Sherr EH, Beckmann ND, Hanson E, Maillard AM, Hippolyte L, et al. A 600 kb deletion syndrome at 16p11.2 leads to energy imbalance and neuropsychiatric disorders. J Med Genet 2012; 49: 660–8.